INVESTIGATION OF SHOWERS PRODUCED BY 45, 130, 230, AND 330 MeV ELECTRONS IN LEAD

O. A. ZAĬMIDOROGA, Yu. D. PROKOSHKIN, [1] and V. M. TSUPKO-SITNIKOV

Joint Institute for Nuclear Research

Submitted to JETP editor April 1, 1966

J. Exptl. Theoret. Phys. (U.S.S.R.) 51, 749-759 (September, 1966)

Showers produced in lead by 45 ± 5, 130 ± 10, 230 ± 15, and 330 ± 20 MeV electrons have been studied with a cloud chamber. Cascade curves and angular distributions of the secondary electrons have been obtained and the track lengths determined.

1. INTRODUCTION

THE study of electron-phonon showers in materials with heavy atoms at low primary-particle energies (hundreds of MeV) presents considerable interest for shower theory, since in this region the cascade theory encounters serious difficulties associated with the strong energy dependence of the cross sections for the elementary electromagnetic processes and the large scattering of the shower particles.

Cascade processes in lead and copper at low energies have been the subject of a number of studies which have provided information on the development of the shower with depth in the medium.[1-5] The purpose of the present study, which was performed with a cloud chamber containing plates, was to study experimentally the showers produced in lead by electrons from 45 to 330 MeV. Very recently several investigations have been made with a similar technique which extend the region studied up to 1 BeV.

2. EXPERIMENTAL ARRANGEMENT

To study electron-photon showers produced by electrons in lead, we used an expansion-type cloud chamber with lead plates, placed in an electron beam.[5] The experiments were performed in 1960 at the synchrocyclotron of the JINR Laboratory for Nuclear Problems. A drawing of the setup is shown in Fig. 1. The electron beam is produced by conversion of γ rays from decay of π^0 mesons produced in the internal target of the synchrocyclotron. A lead converter 4 mm thick was placed in front of a deflecting magnet which separated elec-
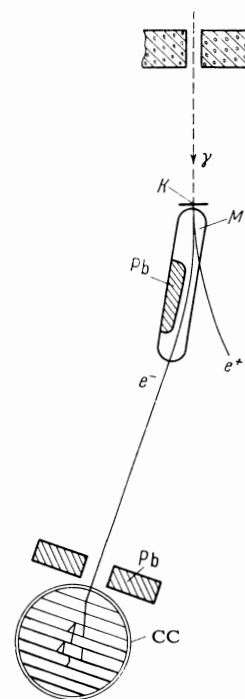

FIG. 1. Experimental arrangement. γ — γ-ray beam, e^- — electron beam, K — lead converter, M — magnet, CC — cloud chamber.

trons of a specified energy. The electron energy was determined by the floating-wire method.[9] The energy spread of the electrons entering the chamber was 5—7%.

The experiment utilized a cloud chamber 40 cm in diameter, similar in construction to that described by Dzhelepov et al.[10] and adapted for operation in the recompression mode.[11] When a large number of plates were used, the recompression method allowed the cycle time of the chamber to be reduced by a factor of 1.5 compared to ordinary operation (to 60 sec). The chamber was filled with a mixture of argon and helium to a pressure

_____

[1] Staff member of the High Energy Physics Institute.

of 1140 mm Hg. The chamber pressure was stabilized by a mercury contact manometer with an accuracy of 2 mm Hg. The liquid used was a mixture of 70% ethyl alcohol and 30% water. The substantial reduction of the chamber sensitive time as a result of the use of plates which increased its interior surface required careful synchronization of the chamber with the accelerator.

Nine lead plates with a total thickness of 50 g/cm² were placed inside the chamber in the path of the beam: four plates each 3 mm thick, two plates 4 mm thick and one plate each of thickness 6, 8, and 10 mm. The height of the plates was 100 mm, and the distance between them 25 mm. The plates were covered with a thin layer of a phenolic varnish.

The chamber was photographed with a stereoscopic camera. Scanning and measurement of the photographs were performed with a stereomagnifier and reprojector.[12]

3. THE EXPERIMENTAL DATA AND THEIR ANALYSIS

The chamber was exposed in the electron beam for four electron energies: 330 ± 20, 230 ± 15, 130 ± 10, and 45 ± 5 MeV. The experimental data to be discussed are based on study of 1003, 321, 634, and 290 showers, respectively.

In the process of development of an electron-phonon cascade, the secondary-particle spectrum changes, becoming softer with increasing distance from the point of origin of the cascade. Therefore all of the characteristics of the cascade process depend substantially on the cutoff energy of the secondary-electron spectrum.[2] Analysis of the multiple scattering of electrons in argon, which comprised 70% of the gas filling the chamber, showed that a definite cutoff energy can be introduced in the spectrum by selection of electron tracks with a definite deviation from the original direction. Figure 2 shows the theoretical mean-square deviation of an electron from the initial direction as a function of the energy and path length of the electron in the chamber gas. It can be seen from the curves of Fig. 2 that for a path length of 25 mm (the distance between the plates) the deflection of an electron from the initial direction becomes appreciable at an energy of 1—1.5 MeV and rises sharply with further decrease of energy. In the analysis of shower photographs, we excluded from analysis tracks with a deviation $l > 3$ mm in
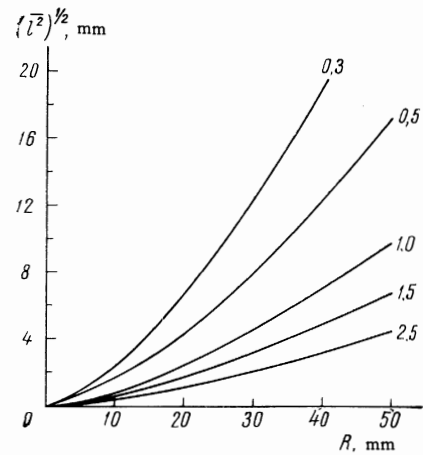

FIG. 2. Mean-square deviation of an electron track $(\overline{l^2})^{1/2}$ as a function of path R in the chamber gas. The numbers on the curves indicate the electron energy in MeV.

a length of 25 mm, which is equivalent to introduction of an effective cutoff energy E = 1—1.5 MeV.

Control measurements showed that visual estimation of the multiple scattering in the scanning provides satisfactory selection of tracks with scattering up to 3 mm in the chamber gap length. In scanning of 426 showers with a primary-electron energy of 330 MeV, all tracks between the plates were divided into three classes: class a)—straight tracks without visible bends; class b)—tracks with noticeable bends, and class c)—electron tracks moving diffusely through the gas. Table I lists the data on the distribution of electron tracks according to these classes in all nine gaps of the chamber.

Figure 3 shows the distributions of electron tracks in the deviation l from the initial direction in a track length of 25 mm for the three classes. The distributions represent the results of measurements in the reprojector of 100 tracks of each
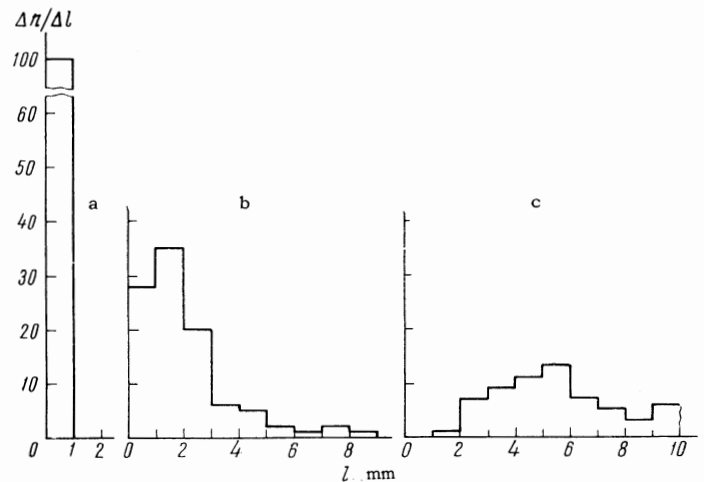

FIG. 3. Distribution of number of electron tracks n as a function of the deviation l in the chamber gaps for track classes a), b), and c).

_____

[2]Here and subsequently we will not distinguish between secondary electrons and positrons.

Table I.

Class of tracks	t, g/cm²								
	3.4	6.8	10.2	13.6	18.1	22.7	29.4	38.6	49.8
a	640	936	1116	1127	1051	881	600	381	251
b	11	31	63	69	81	81	35	56	41
c	23	24	59	96	82	106	142	127	94

class. It is evident from the distributions that all tracks of class a) have a deviation of not more than 1 mm, for class b) only 15% of the tracks have a deflection greater than 3 mm, and for class c) 10% of the tracks have a deviation less than 3 mm. It follows from this that tracks of class c) belong mainly to electrons with energy below 1 MeV, so that selection of events of classes a) and b) corresponds to introduction of a cutoff of the spectrum at a level $E = 1-1.5$ MeV. The error due to the uncertainty in such a classification of the tracks is considerably less than the statistical error for most of the gaps and approaches it only in the last gaps of the chamber. However, for these gaps the error due to corrections for detection efficiency and background are several times greater than the statistical error.

4. CASCADE CURVES

The cascade curves $N(E_0, E, t)$ obtained—the average number of electrons and positrons with energy greater than E at a depth t in the absorber—are shown in Fig. 4 for four values of primary electron energy E_0, for $E = 1$ MeV. In the experimental distributions we have introduced a correction for the geometrical inefficiency due to the lateral divergence of the shower and the finite dimensions of the primary-electron beam. To determine the corrections we selected 134 showers with a primary energy of 330 MeV in frames with minimum background. For these showers we meas-

ured the coordinates of the points of exit of the electrons from the plates, with respect to the shower axis. The lateral distribution of secondary electrons obtained in this way allowed us to determine the average efficiency for detection of electrons for each gap. The efficiency for detection of tracks in a shower from 330-MeV electrons, whose axis was near the middle of the illuminated zone, was 100% for the first three gaps and decreased to 60% for the last gap.

In addition, from the lateral distribution of the points of exit of electrons from the plates we estimated the background from showers which developed outside the illuminated zone. The background due to the operation of the accelerator and the background of natural radioactivity of the chamber materials were determined by photographing the chamber with no converter in the γ-ray beam.

The cascade curves shown in Fig. 4, when plotted on a semilogarithmic scale, are closely fitted by straight lines in the region beyond the peak. The absorption coefficients τ calculated by the method of least squares have values of -0.050 ± 0.003, -0.048 ± 0.003, -0.056 ± 0.004, and -0.10 ± 0.01 cm²/g for energies of 330, 230, 130, and 45 MeV, respectively.

Blocker, Kenney, and Panofsky[1] showed that in lead 40% of the total ionization at the peak of the shower is produced by electrons scattered backwards. In order to make a qualitative estimate of the contribution of these electrons for a part of the
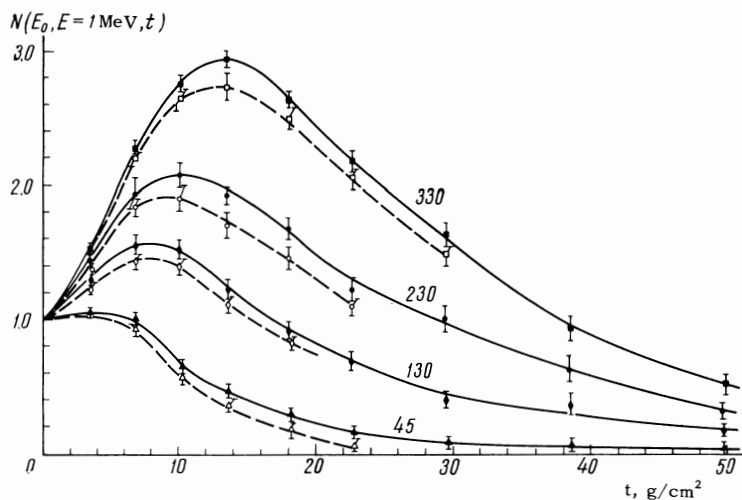

FIG. 4. Cascade curves $N(E_0, E = 1$ MeV, t). The values of E_0 in MeV are indicated on the respective curves. The solid points are cascade curves taking into account all electrons with energy greater than 1 MeV, and the hollow points are cascade curves not taking into account secondary electrons scattered backwards.
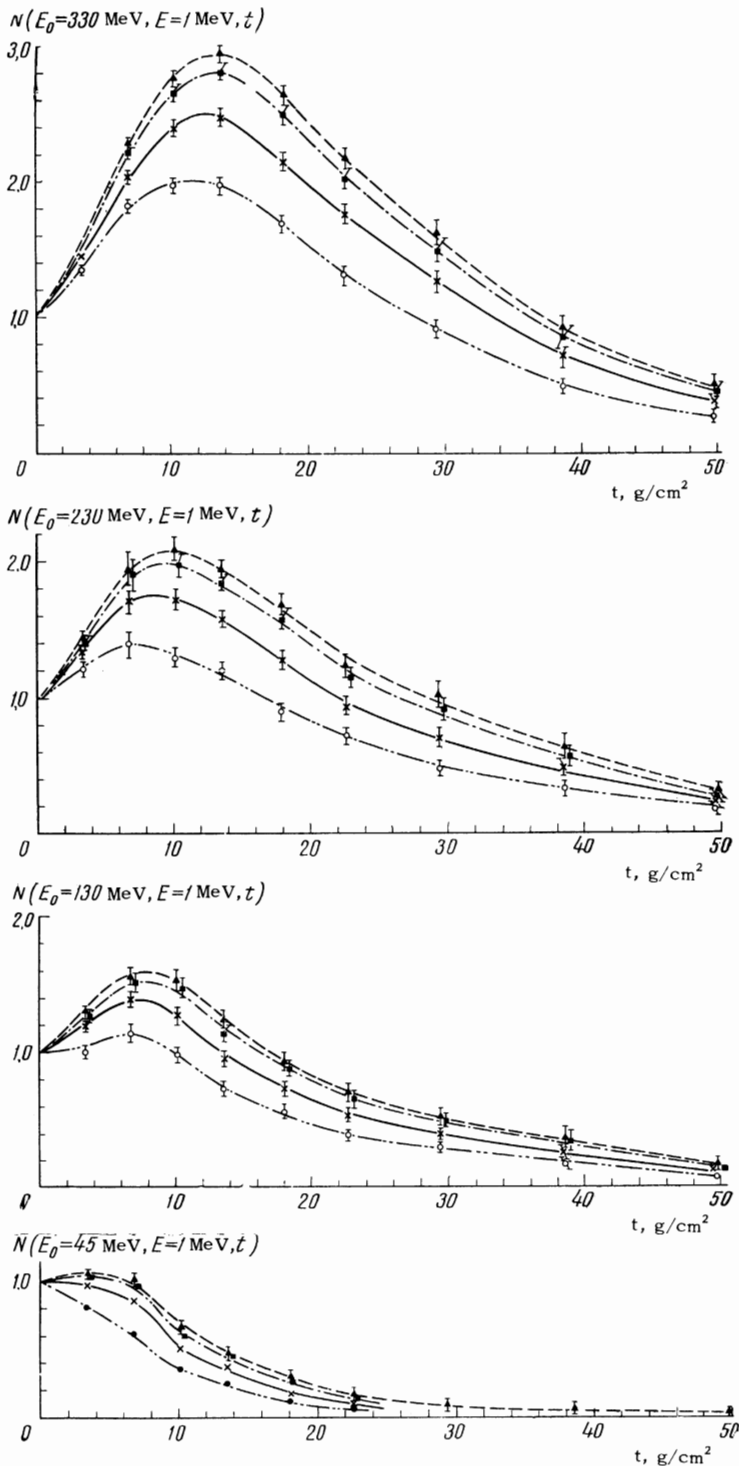
FIG. 5. Cascade curves for different maximum emission angles of secondary electrons: ▲ – $\theta \leq 90°$, ■ – $\theta \leq 60°$, × – $\theta \leq 45°$, ○ – $\theta \leq 30°$, and for four values of primary-electron energy E_0.

showers, we introduced additional selection criteria—tracks of particles scattered backwards with respect to the shower axis were not counted. The numbers of showers for energies of 330, 230, 130, and 45 MeV were respectively 426, 254, 303, and 268. For thicknesses greater than 20—30 g/cm^2, because of the increased angular and spatial divergence of the shower particles, the possibility of separating back-scattered electrons in the multiplate chamber was reduced. Figure 4 shows cascade curves plotted for these showers. It can be seen from this figure that the fraction of backscattered electrons amounts to about 10% in the region of the peak in the cascade curve and increases rapidly with absorber thickness.

To obtain information on the angular divergence of the shower particles, we measured the electron emission angles θ with respect to the shower axis for all the gaps. Figure 5 shows cascade curves for various maximum values of θ.
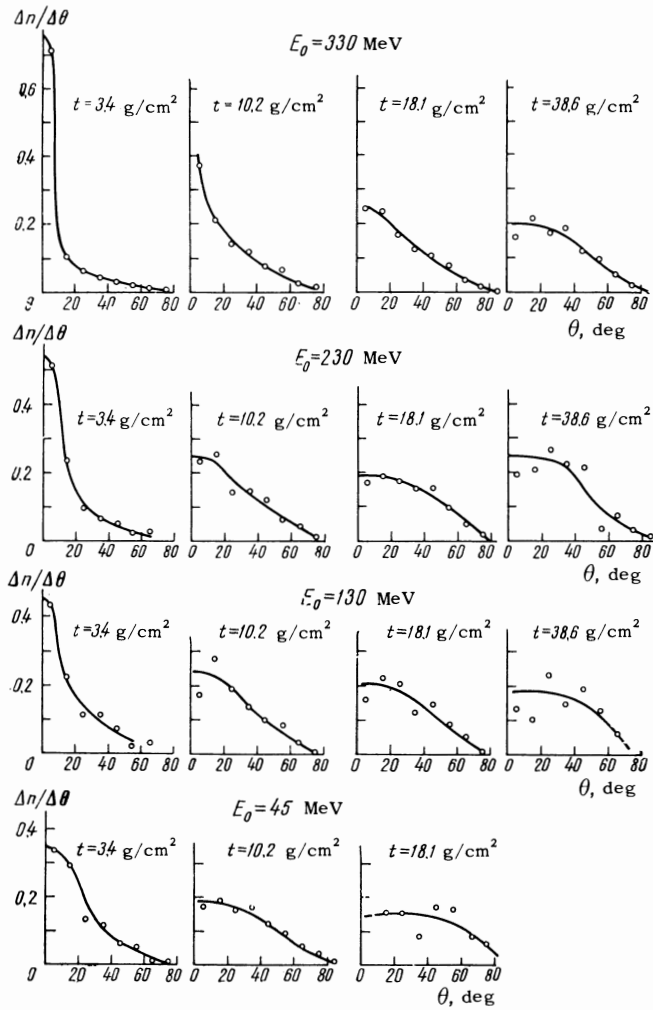
FIG. 6. Distribution of numbers of electron tracks n as a function of angle θ.

FIG. 7. Average values $\overline{\sec \theta}$ at different shower depths t. The values $\overline{\sec \theta}$ averaged over the entire shower for energies of 330, 230, 130, and 45 MeV are respectively $\langle \overline{\sec \theta} \rangle$ = 1.24, 1.30, 1.25, and 1.29.

by extrapolation of the cascade curves on the basis of the values of absorption coefficient found for them.

5. DISCUSSION OF RESULTS

Figure 8 shows the cascade curves obtained in present work for 45—330 MeV primary electrons, together with the data of other studies performed in the same energy region.[6,8]

In the first of these studies, which was carried out with a propane chamber, the cutoff energy of the secondary-particle spectrum also amounted to about 1 MeV.[6] In the second study, carried out with a multiplate cloud chamber,[8] a cutoff energy of the recorded electron spectrum was not introduced directly in obtaining the cascade curves. The track selection criteria reduced to recording tracks with an effective polar angle not greater than 60° with respect to the shower axis, and recording tracks of particles passing close to the shower axis and which are not scattered in the gas. The selection in[8] of tracks without noticeable scattering in the gas corresponds to a secondary-electron cutoff energy E of about 1 MeV, i.e., also close to that introduced in the present work.

The data of the present work (Fig. 5) show that the difference in the cascade curves for detection of all secondary electrons and only of electrons

Figures 6 and 7 show the angular distributions of secondary electrons as a function of absorber thickness t for four values of primary particle energy.

An important characteristic of the cascade process is the integral track length

$$I(E_0, E) = \int_0^\infty N(E_0, E, t)\, dt.$$

The integral track length is related to the primary-particle energy by the simple relation

$$E_0 = \epsilon I(E_0, E)\overline{\langle \sec\theta \rangle} / p(E_0, E) = g(E_0, E) I(E_0, E). \quad (1)$$

where ϵ is the critical energy, and t is measured in radiation lengths; $p(E_0, E)$ takes into account the introduction of a cutoff energy, and the averaged secant $\langle \sec\theta \rangle$ takes into account the angular divergence of the electrons (see Fig. 7).

Table II lists the values of $I(E_0, E = 1 \text{ MeV})$ obtained for four values of primary-electron energy. The integrals of the cascade curves were computed
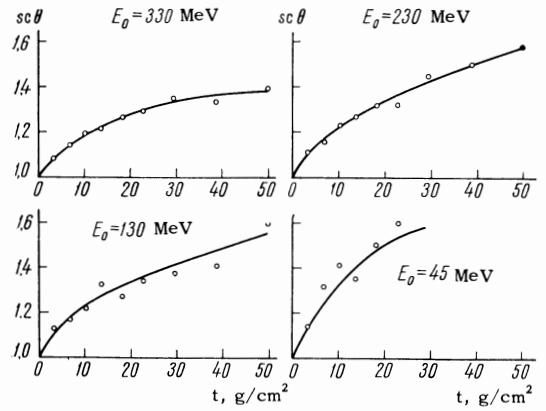
Table II.

E_0, MeV	J, g/cm^2	$I(E_0, E=1 \text{ MeV})$, g/cm^2	$g(E_0, E=1 \text{ MeV})$, MeV-cm^2/g
330	85.4	96.3	3.43
230	57.8	64.8	3.55
130	38.6	41.6	3.13
45	16.8	17.2	2.62

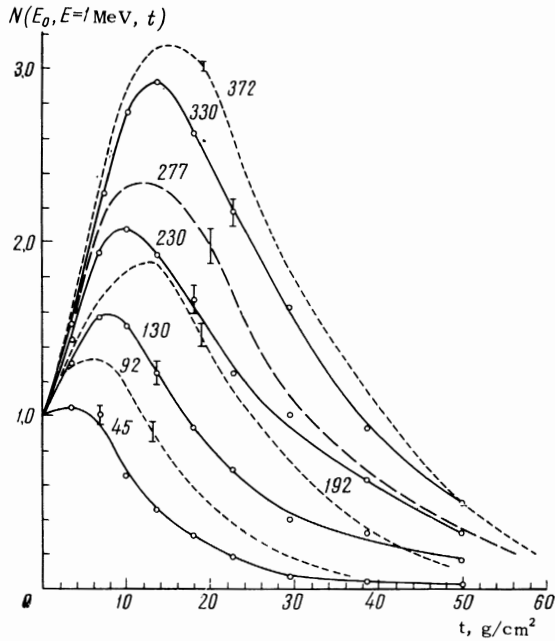Here $J = \int_0^{50} N(E_0, E = 1 \text{ MeV}, t)\, dt$.

FIG. 8. Cascade curves for different primary-electron ener-gies E_0. The values of E_0 in MeV are shown by the numbers on the curves. Typical experimental errors are shown in the fig-ure. The data for E_0 = 92, 192, and 372 MeV were taken from [6], and for E_0 = 277 MeV – from [8].

FIG. 9. Shower track length $I(E_0,E)$ as a function of pri-mary-electron energy E_0: ● – present work, □ – [6], △ – [7], ◇ – [8].

According to the data of Table I, the track length I for low-energy electrons (class c)) amounts to about 30% of the value of $I(E_0, E = 1$ MeV) found for classes a) and b). It follows from this that the average energy loss of these electrons is four times the ionization loss of the relativistic elec-trons of the shower, and the average energy of the "soft" electron component of the shower ($E < 1$ MeV) is about 0.1 MeV. This conclusion agrees with the results of computations by Craw-ford and Messel.[15]

The shower calculations made up to the present time by the Monte Carlo method are rather frag-mentary in nature, and the possibilities of com-paring our data with the results of these calcula-tions are limited. Figure 10 shows a cascade curve obtained from the data of the present work (E_0 = 200 MeV, E = 1 MeV, t) and curves calculated for E_0 = 200 MeV and E = 1.5 and 2.5 MeV.[16] Also shown here for comparison is a cascade curve calculated with a high cutoff energy E = 10 MeV.[15] We can see from the figure that the difference between the theoretical values of the cascade curve and the experimental values does not exceed 20%. If we consider the difficulties in calculating the shower for low secondary-particle energies and the uncertainty in the cutoff energy, this agreement must be considered good.

whose tracks lie in a cone $\theta \lesssim 60°$ is small in the region $t \lesssim 40$ g/cm^2. This allows us to compare the cascade curves shown in Fig. 8, without introduc-ing any important corrections. It is evident from Fig. 8 that the data of all three studies are in satis-factory agreement.

The track length $I(E_0, E)$ is shown in Fig. 9 as a function of primary-electron energy, according to the data of the present work and of other studies made by means of track chambers.[6-8] It can be seen from this figure that the track length is a linear function of the primary-electron energy over a primary-electron energy range from 45 to 1000 MeV (see also[13]).

The average value of the coefficient $g(E_0, E = 1$ MeV) in formula (1), according to the data of the present work (Table II) and of other studies[6-8] made in the energy region up to 400 MeV, is 3.3 ± 0.4 MeV-cm^2/g or 21 MeV if t is measured in radiation lengths (6.4 g/cm^2 [14]). Using the known values $\langle \overline{\sec\theta} \rangle \approx 1.3$ (Fig. 7) and the critical energy $\epsilon = 7.4$ MeV,[14] we obtain

$$p(E_0. E = 1 \text{MeV}) = 0.46 \pm 0.10.$$

Thus, the energy dissipated in the course of a shower by ionization loss of electrons with E > 1 MeV amounts to only half of the total energy of the shower. The remainder of the shower energy is dissipated by electrons with energy below 1 MeV.
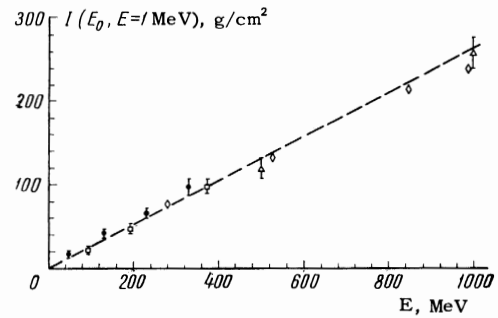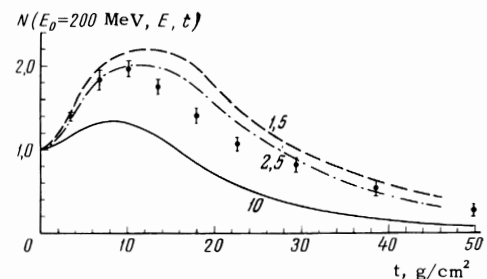

FIG. 10. Comparison of the experimental cascade curve N(E_0 = 200 MeV, E = 1 MeV, t) with theoretical results [15,16] obtained for various energies E. Values of E are shown on the curves (in MeV).

Comparison of the experimental cascade curves (present work and data of[6-8]) with the results of calculations by the method of moments[17] can as yet be made only indirectly, since these calculations were made for showers produced by γ rays rather than by electrons.[18] This comparison can be made most conveniently for the track lengths of the showers, since according to the calculations of Richards and Nordheim[19] the track lengths of showers produced by electrons and γ rays are nearly the same for the case $E_0 \gg E$. For the cascade curves calculated by the method of moments,[18] $g(E_0, E = 1 \pm 0.5$ MeV$) = 1.8 \pm 0.25$ MeV-cm^2/g. This value is smaller than the experimental value 3.3 ± 0.4 MeV-cm^2/g.

[1] W. Blocker, R. W. Kenney, and W. K. H. Panofsky, Phys. Rev. **79**, 419 (1950).

[2] W. E. Hazen, Phys. Rev. **66**, 254 (1944).

[3] A. Kantz and R. Hofstadter, Nucleonics **12**, 36 (1954).

[4] P. A. Bender, Nuovo Cimento **2**, 980 (1955).

[5] Yu. D. Prokoshkin, and T'ang Hsiao-wei, JETP **36**, 10 (1959), Soviet Phys. JETP **9**, 6 (1959).

[6] H. Lengeler, W. Tejessy, and M. Deutschmann, Z. Physik **175**, 283 (1963).

[7] E. E. Becklin and J. A. Earl, Phys. Rev. **136**, B237 (1964).

[8] H. Thom, Phys. Rev. **136**, B447 (1964).

[9] M. S. Kozodaev and A. A. Tyapkin, PTÉ, **1**, 21 (1956).

[10] V. P. Dzhelepov, M. S. Kozodaev, V. T. Osipenkov, N. I. Petrov, and V. A. Rusakov, PTÉ, **3**, 3 (1956).

[11] E. R. Gaerttner and M. L. Yeater, Rev. Sci. Instr. **20**, 588 (1949).

[12] A. T. Vasilenko, M. S. Kozodaev, R. M. Sulyaev, A. I. Filippov, and Yu. A. Shcherbakov, PTÉ, **6**, 34 (1957).

[13] Yu. D. Prokoshkin and T'ang Hsiao-wei, PTÉ, **3**, 32 (1959).

[14] O. I. Dovzhenko and A. A. Pomanskiĭ, JETP **45**, 268 (1963), Soviet Phys. JETP **18**, 187 (1964).

[15] D. F. Crawford and H. Messel, Phys. Rev. **128**, 2352 (1962).

[16] H. H. Nagel and Ch. Schlier, Z. Physik **174**, 464 (1963).

[17] S. Z. Belen'kiĭ and I. P. Ivanenko, UFN **69**, 591 (1959), Soviet Phys. Uspekhi **2**, 912 (1960).

[18] I. P. Ivanenko, JETP **32**, 491 (1957), Soviet Phys. JETP **5**, 413 (1957).

[19] J. A. Richards and L. W. Nordheim, Phys. Rev. **74**, 1106 (1948).